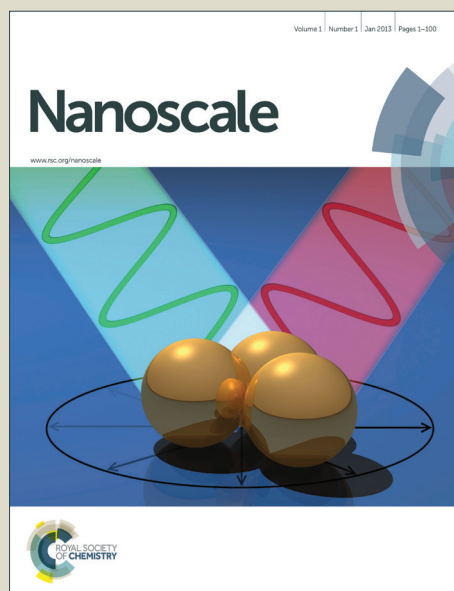


Nanoscale

Accepted Manuscript



This is an *Accepted Manuscript*, which has been through the Royal Society of Chemistry peer review process and has been accepted for publication.

Accepted Manuscripts are published online shortly after acceptance, before technical editing, formatting and proof reading. Using this free service, authors can make their results available to the community, in citable form, before we publish the edited article. We will replace this *Accepted Manuscript* with the edited and formatted *Advance Article* as soon as it is available.

You can find more information about *Accepted Manuscripts* in the [Information for Authors](#).

Please note that technical editing may introduce minor changes to the text and/or graphics, which may alter content. The journal's standard [Terms & Conditions](#) and the [Ethical guidelines](#) still apply. In no event shall the Royal Society of Chemistry be held responsible for any errors or omissions in this *Accepted Manuscript* or any consequences arising from the use of any information it contains.

Tempo-spatially Resolved Cellular Dynamics of Human Immunodeficiency Virus Transactivating Activator of Transcription (Tat) Peptide-modified Nanocargos in Living Cells

Lin Wei, Qiaoyu Yang, and Lehui Xiao*

Key Laboratory of Chemical Biology & Traditional Chinese Medicine Research,
Ministry of Education, Key Laboratory of Phytochemical Research and Development of
Hunan Province, College of Chemistry and Chemical Engineering, Hunan Normal
University, Changsha, Hunan, 410081, P. R. China.

KEYWORDS

Tat peptides, gold nanoparticles, darkfield microscope, optical imaging, nanocargos

ABSTRACT

Understanding the cellular uptake mechanism and intracellular fate of nanocarriers in living cells is of great importance for the rational design of efficient drug delivery cargos as well as the development of robust biomedical diagnosis probes. In this work, with a dual wavelength view darkfield microscope (DWVD), the tempo-spatially resolved dynamics of Tat peptide-functionalized gold nanoparticles (TGNPs, with size

similar to viruses) in living HeLa cells were explored extensively. It was found that energy-dependent endocytosis (both clathrin and caveolae mediated processes were involved) was the prevailing pathway for the cellular uptake of TGNPs. The time-correlated dynamic spatial distribution information revealed that TGNPs couldn't actively target the cell nuclei, which is contrary to previous observations based on fixed cell results. More importantly, inheritance of TGNPs to the daughter cells through mitosis was found to be the major route to metabolize TGNPs by HeLa cells. These understandings on the cellular uptake mechanism and intracellular fate of nanocargos in living cells would provide deep insight on how to improve and controllably manipulate the translocation efficiency for targeted drug delivery.

INTRODUCTION

Development of nonviral nanocargos for gene and drug delivery has aroused considerable attention in nanomedicine over past years. A wide range of nanomaterials have found to be good carriers in living cells, such as carbon nanotubes, liposomes, mesoporous silica nanoparticles, gold nanoparticles and so on.¹⁻⁴ Among these functional nanocarriers, gold nanoparticles received more attention because of their attractive optical features, biocompatibility and versatile surface chemistry.⁴⁻⁷ The pioneering studies have demonstrated to deliver many types of biomolecules into living cells with gold nanoparticles but displaying variable efficiencies.⁸⁻¹¹ Further investigations revealed that different combinations of size, shape and surface coating usually result in the nanocargo exhibiting very complex physicochemical features that significantly influence the cellular uptake efficiency.¹²⁻¹⁵ To reach full potential in biomedical applications, a general yet robust method is desired for the efficient delivery of nanocargos into living cells.

A promising solution to this grand challenge is cell-penetrating peptides (CPPs), which are typically composed of positively charged short amino acid sequences.¹⁶⁻¹⁹ Functionalization of CPPs to the nanocargo surface can greatly facilitate cellular uptake of different types of cargos from nanosize particles to small chemical molecules and even impermeable biomolecules.²⁰⁻²³ Transactivating activator of transcription (Tat) peptide from Human Immunodeficiency Virus 1 (HIV-1) is one of the most commonly studied CPPs. Several studies have shown that covalent conjugation of Tat peptides to gold nanoparticles with different size or shape all exhibited unprecedented cellular uptake efficiency in various cell lines.²⁴⁻²⁶ Despite these great achievements, so far, there is still

lacking of satisfactory model with predictive power on the mechanism of how Tat peptide-functionalized nanocargos are internalized and metabolized by living cells. Even for the simplest system (e.g., single peptide), various complicated cellular uptake mechanisms are proposed owing to the ability of any biological system to react to external and internal stimuli with a complex response.^{19,27-29}

In nanomaterial-based drug delivery system, it has been recognized that, the drugs or functional materials have to be released into cytosol or be delivered to specific subcellular organelles for the improvement of drug transportation and drug action, reduced drug dosage, and minimized drug side effect.³⁰⁻³³ Otherwise, the potential biomedical usefulness of drugs would be limited, since those reagents would never participate in any cytosolic or organelle-based events. Until now, the knowledge of cellular uptake mechanism and intracellular fate of Tat peptide-functionalized nanocargo is still at the stage of information gathering. There have fruitful yet debatable scenarios been proposed on this concern so far.^{26,34-38} For example, several reports demonstrated that most of the nanoparticles are taken up by cells via endocytosis and generally confined in the endocytic vesicles until they are eventually cleared by exocytosis.^{34,38} Alternatively, there are some experimental results also showed that distinct cellular uptake mechanisms involve the ability of the nanoparticles to enter into the cytosol and even exhibit the capability to specifically target the cell nucleus.^{25,26,36}

Clearly, from the point of building up new generation efficient drug carriers, it is of great importance to develop a full and detailed understanding of the complex processes that govern the cellular uptake and intracellular fate of Tat peptide-functionalized nanocarriers. So far, several methods have been adopted to investigate the cellular fate of

Tat peptide-functionalized gold nanoparticles (TGNPs), such as TEM, silver enhanced staining and so on.^{26,36,39} Although TEM results can provide high spatial resolution information about the intracellular distribution; a critical limitation is that the knowledge is not directly elucidated in-situ. During the time-consuming cell fixing process, additional errors might be introduced.¹⁹ A more convincing strategy to comprehend the interesting yet complicated cellular dynamics of TGNPs is to track their motions in living cells in real time.

In this work, by taking the advantage of the localized plasmon resonance property of gold nanoparticles, we explored the dynamics of TGNPs in living cells with dual wavelength view darkfield microscope (DWVD).⁴⁰ Several remarkable conclusions were drawn based on the tempo-spatially resolved microscopic imaging results. From the comprehensive control experiments, it was demonstrated that TGNPs entering into HeLa cells were basically guided by energy-dependent endocytosis (both clathrin- and caveolae-mediated were involved). The internalized TGNPs were predominantly confined inside the endocytic vesicles. No membrane rupture was observed. Alternatively, motor proteins guided continuous fusing and splitting on cellular cytoskeletons were the dominant routes causing TGNPs-loaded vesicles aggregation and redistribution inside the living cells, which also resulted in apparent nuclear targeting during the mitosis process. More interestingly, inheritance of TGNPs to daughter cells was found to be the dominant pathway to metabolize TGNPs by HeLa cells.

RESULTS AND DISCUSSION

Fabrication and characterization of TGNPs.

Previous investigations have revealed that the shape, size, surface charge as well as coating of drug carriers are the major factors controlling the cellular uptake efficiency.^{12,14,41} From the perspective of size effect, it was demonstrated that a spherical nanoparticle with diameter around 50 nm would exhibit the highest efficiency for cellular internalization owing to the favorable size dimension for membrane curvature generation.⁴² In this consideration, we chose 60 nm spherical gold nanoparticles (60 ± 2.5 nm based on TEM measurement) as a model system to investigate the cellular uptake mechanism as well as the tempo-spatial distribution of TGNPs in living cells.

Since the experiments will be performed in cell culture medium and inside living cell where high salt concentration and complicated biomolecules will exist, a good colloidal stability should be the primary requirement for TGNPs in this study. Besides, another important consideration is the stability and biological functionality of Tat peptides after being coated on the nanoparticle surface. These two fundamental requirements are satisfied through the modification strategies as shown in Figure 1. By taking the advantage of versatile gold-thiol chemistry, we anchored Tat peptides on the surface of gold nanoparticles with a NHS functionalized PEG linker (SH-PEG-NHS, with a thiol group on the other end). This design exhibits two noticeable benefits. Firstly, because of the covalent gold-thiol linkage, Tat peptides can be stably attached on the gold nanoparticle surface even in cell culture medium. Secondly, the spacer (PEG) can shield the direct interaction between Tat peptides and gold nanoparticle surface, which thus maintains the native biological function of Tat peptides. In addition to the stability of Tat

peptides, nonspecific binding of biomolecules on the nanoparticle surface might complicate the biological functionality of Tat peptides. To handle this issue, another thiolated PEG molecule (SH-PEG-CH₃) was introduced to block those remaining anchoring sites on gold nanoparticle surface.

A set of comprehensive characterizations was applied to estimate the stability of TGNPs and the performance of biological modification process. Since the resonant scattering condition of plasmonic nanoparticles is very sensitive to the dielectric constant of the surrounding close to the nanoparticle, UV-vis absorption spectrum can then be utilized to confirm the modification process. Figure 1b shows the typical UV-vis spectra of 60 nm gold nanoparticles before and after Tat peptides modification. As indicated in the inserted plot, a 3 nm red shift can be readily found after the modification process, indicative of the successful conjugation of Tat peptides on the gold nanoparticle surface.³⁷ The increased zeta potential from -32 mV to -20 mV further confirms this point.

Then we explored the colloidal stability of TGNPs in cell culture medium and different salt concentrations. Since the objective of this investigation is to explore the tempo-spatially resolved dynamics of TGNPs in living cells, it is more interesting to statistically evaluate the stability of the nanocargo at single particle level rather than ensemble spectroscopic measurement. It is well known that the scattering cross-section of plasmonic nanoparticles scales as a function of the six power of their radius.⁴³ Thus, the scattering intensity of individual object in the darkfield image is a sensitive and accurate criterion to assess the stability and dispersiveness of TGNPs.^{37,44} The statistical distributions of scattering intensity from individual spots in different surroundings are

shown in Figure 1c. The particles modified according to above described strategy exhibited superior stability over a broad range of salt concentrations as well as in cell culture medium, indicative of a stable linkage between gold nanoparticles and ligands on the surface. In sharp contrast, the particles without modification were aggregated rapidly within 5 mins even in 50 mM NaCl solution, Figure S1.

Diffusion dynamics of TGNPs on cell membrane.

With a standard darkfield microscope, it is difficult to differentiate individual gold nanoparticles with size down to 100 nm in living cells.^{40,45} The major obstacle is the strong background noise from cellular organelles owing to the mismatch of refractive index between subcellular organelles and cell cytosol. Since the elastic scattering efficiency of cellular organelles is typically insensitive to the wavelength of light source over a broad range as observed in our previous experiment, it is therefore possible to differentiate small size gold nanoparticles from cellular background with a DWVD imaging modality based on the benefit of plasmon resonance effect of TGNPs, Figure 2.⁴⁰

Earlier works have shown that either energy-dependent (endocytosis) or -independent processes (such as direct penetration) are adopted by living cells for the internalization of CPPs, where the peptide-membrane interaction plays a dominant role on this process.^{19,27-29} Exploring the diffusion dynamics of TGNPs on cell membrane would therefore afford insightful information on the accurate elucidation of cellular internalization mechanism. In this regard, we tracked the membrane dynamics of individual TGNPs with DWVD. Interestingly, those trapped nanoparticles on cell membrane were not firmly adhered on the initial contact points. The majority of TGNPs were diffusing on the cell membrane at a relatively long-range scale with a slowed

diffusion coefficient of $0.003 \pm 0.001 \text{ } \mu\text{m}^2/\text{s}$, Figure 3. This kind of long-term and large-scale lateral diffusion is notably distinct from that of CTAB-modified gold nanoparticles (positively charged with the same size), Figure S2. In this control, the nanoparticles were effectively confined at the initial anchoring sites without noticeable lateral diffusions.

It is worth noting that the isoelectric point of Tat peptide is around 12. In cell culture medium, TGNPs might exhibit a tendency to spontaneously assemble onto the negatively charged cell membrane via electrostatic associations. In other words, the membrane association process would not be the rate-limiting step in consideration of the vigorous thermal diffusion. Since this kind of association is recognized to be mainly regulated by thermal diffusion, the cell membrane can thus provide even opportunity for the internalization of trapped nanoparticles at any anchoring site as noted in the control (CTAB-modified nanoparticles).

Obviously, the scenario based on electrostatic association cannot well account for the above observations. The long-range membrane diffusion indicates a heterogeneous membrane environment where TGNPs have to diffuse and then survey suitable anchoring sites for the concomitant penetration process. Even though the electrostatic interaction can promote the adsorption process, it is still not sufficient to directly guide the nanocargo in crossing the cell membrane. Further inspection of the lateral diffusion trajectories led to an interesting observation that the majority of nanocargos underwent noticeable hop diffusions as shown in Figure 3b. This behavior is remarkably distinct from that in the control experiment (Figure S2) as well as the behavior of single Tat peptides on lipid membrane (confined random diffusion).⁴⁶ The anchoring time at each step varies from time to time, indicative of heterogeneously distributed interaction

strength not only in the spatial region but also in the temporal domain. Meanwhile, by statistically analyzing the step size from individual particles, an apparent asymmetric distribution can be readily observed, confirming a non-Brownian diffusion mode, Figure 3b. This kind of diffusion is analogous to previous observations from transferrin-modified nanocargo on living cell membrane (ligand-guided endocytosis pathway) and is also different from the confined random diffusion of Tat peptides on model lipid membrane.^{46,47} The above observations give rise to a strong point that the cellular uptake of TGNPs is not guided by pure energy-independent physical association and penetration. This argument is further confirmed by the following control experiments.

Cellular uptake mechanism.

It is well known that hydrophilic substances passing through the hydrophobic plasma or cell membrane is a kinetically unfavorable process. For living cells, endocytosis is the dominant pathway to import external substances. To determine the key factors regulating the cellular uptake process of TGNPs, HeLa cells were co-incubated with TGNPs at 4 °C where the energy-dependent endocytic process would be inhibited due to the deactivation of ATPase.⁴⁸ As shown in Figure 4, a drastic inhibition of internalization was observed in contrast to that at 37 °C, indicating that energy-dependent endocytosis plays a dominant role on the cellular uptake process. It is worthy of note that HeLa cells are typically considered as nonphagocytosing cells, the inhibition of particle internalization by deactivation of ATPase may reflect inhibition of either clathrin- or caveolae-mediated endocytosis, or a combination of these two.¹³

In order to more clearly comprehend the role of specific endocytic pathway, the HeLa cells were treated with two well known biochemical inhibitors for endocytosis

processes, Dynasore (an inhibitor of clathrin-mediated endocytosis by deactivating dynamic-GTPase) and genistein (an inhibitor of caveolae-mediated endocytosis by deactivating isoflavone tyrosine kinase).^{13,49} As shown in Figure 4c, when HeLa cells were treated with Dynasore, an obvious suppression of internalization was observed in comparison with that without drug treatment. Analogous inhibition effect was also noted in the genistein control, Figure 4d. However, despite the reduced uptake efficiency, few TGNPs could still be distinguished inside the cell. No complete inhibition was found in these two controls as that in the temperature control experiment. All of these observations lead to a strong argument that both clathrin- and caveolae-mediated endocytosis might involve in the uptake process. To confirm this assumption, we treated HeLa cells with Dynasore and genistein simultaneously. In this control, given the above hypothesis is valid, we then expect to observe a more effective inhibition of cellular internalization. As demonstrated in Figure 4e, remarkable inhibition was found which is reminiscent of the temperature control. Taken together, the above experimental results clearly suggest that the cellular internalization of TGNP by HeLa cell is regulated in a complex way where both clathrin- and caveolae-mediated endocytosis processes are involved.

Clustering and redistribution of TGNPs inside HeLa cells.

Once the nanocargo was delivered into living cell, two important concerns should be addressed: how it moves inside the cell and where it finally locates after a complete cell cycle. These two messages are fundamentally important because the fate of those nanocargos will finally determine their biomedical functionality. With DWVD, the spatial distribution of internalized TGNPs within living cell can be recorded in a non-invasive way (i.e. three-dimensional section imaging), Figure S3. As time goes on, the

number of nanoparticles on cell membrane increased gradually. Around one hour later (after the TGNPs was added to the culture dish), individual TGNPs appeared inside the cytosol, Figure S3. In order to selectively and continuously track the intracellular dynamics and map the fate of those internalized nanocargos, we chose one hour as a dead point for the co-incubation process. Those excess nanoparticles in solution or nonspecifically and loosely adsorbed on the cell membrane were then washed away with cell culture medium.

Figure 5 shows a set of time evolution images at different time points. Before 3 h, most of TGNPs were distributed around the cell and the scattering intensity from those spots was relatively homogeneous, indicating that the cellular translocation process of TGNPs favors a monomer way. This observation is in good agreement with previous experimental results by using transferrin-coated gold nanoparticle as the probe.⁴¹ A clear transition point could be observed at around 6 h. Noticeable aggregated clusters were gradually found around the cell and the scattering intensity from them was not homogeneously distributed. These results demonstrate that the movement of nanoparticles within the cell is not regulated by thermal diffusion while they can still gradually aggregate in a heterogeneous manner as time goes on. This kind of aggregation notably deviates from the mechanism of either diffusion-controlled or reaction-limited self-aggregation.⁵⁰ More importantly, the internalized nanoparticles were still randomly distributed around the cell even 6 h later. No active nuclear targeting effect was observed, which is apparently contrary to the previous observations.²⁵

Interestingly, around 12 h later, the aggregated clusters were concentrated around the cell nuclei and the size of those clusters became much bigger. However, this kind of

targeting is not stable. The concentrated clusters could again scatter toward the outer sphere of membrane as shown at around 18 h. No further nuclear targeting was observed until 36 h (after a complete cell cycle) except the slowly increased cluster dimension. This periodic nuclear targeting process gives rise to a strong argument that those particles within the living cells cannot actively target cell nuclei by thermal diffusion.

According to above results, it is thus significant to explore why these TGNPs cannot actively target HeLa cell nuclei? In order to address this question, we tracked the intracellular dynamics of individual internalized objects. As shown in Figure S4, those particles were either moving in a directed fashion or confined within a vesicle. Thermal energy induced random diffusion within the cell was not observed. These observations are well consistent with the above conclusion that endocytosis is the dominant pathway for these TGNPs. After the endocytosis process, the majority of particles were still confined within endocytic vesicles, which effectively froze their thermal diffusion and might guide them move along microtubules (directed movements). This argument is further confirmed by labeling the endosomes with acridine orange (a dye that is used to label acidic endosomes).⁵¹ As shown in Figure S5, the majority of internalized TGNPs within HeLa cell could be co-localized with acridine orange labeled acidic vesicles. However, it is very strange why those trapped nanoparticles could gradually aggregated within the living cell? Further inspection of the dynamics of individual objects, an interesting observation was found that motor proteins directed movements on microtubules exhibited a tug-of-war behavior, causing different endocytic vesicles fusing together or splitting away, which clarifies the heterogeneous aggregation process for these internalized TGNPs, Figure 6. This kind of real time dynamics are difficult to be

elucidated with other static measurements such as TEM or SEM.^{36,39} Furthermore, these observations also confirmed that the apparent nuclear targeting effect from TGNPs is not an active targeting process initiated by Tat peptides, which is actually regulated by motor proteins (or the cell itself). At different cell cycles, motor proteins will guide the nanoparticles transport on the cell cytoskeletons toward specific directions. Therefore, more attention should be paid to interpret the intracellular fate of functionalized nanoparticles when using static characterization methods.

Besides the tempo-spatially resolved distribution information, another important question is the metabolic mechanism of TGNPs by living cells, which has also aroused great debates recently. Some evidences have shown that the nanoparticles taken up by endocytosis are generally confined in endocytic vesicles until they are eventually cleared by exocytosis.^{26,41,52} To explore whether similar manner was adopted herein; atomic absorption spectrum (AAS) is applied to monitor the fluctuation of gold content within HeLa cells. We firstly co-incubated TGNPs with several batches of HeLa cells for 1 h in serum-free DMEM. The content of TGNPs remained in cell culture medium were washed out and determined with AAS. Then, TGNPs-loaded HeLa cells were supplemented with fresh culture medium and incubated for different time scales. The content of TGNPs inside or excreted by HeLa cells at different time points were determined by digesting HeLa cells or the fresh culture medium in aqua regia respectively. Provided the particles could be excreted via exocytosis, the content of particles in fresh cell culture medium should gradually increase as a function of time while those inside HeLa cells should be decreased concomitantly. As shown in Figure 7, the content of TGNPs within HeLa cells didn't change as a function of time, which is also consistent with the results from original

cell culture mediums. No detectable TGNPs were found in the fresh culture mediums (comparable to the baseline), if any. These results directly indicate that the internalized TGNPs were mainly kept inside the cell even after a complete cell cycle (see the results 24 h later). Exocytosis was not adopted in this case. The microscopic imaging result further confirms this conclusion, Figure 5, where no observable particle was detected around the cell periphery even 24 h later. Based on these experimental results, it is reasonably to propose that inheritance of nanoparticles to the next generation cells should be the dominant pathway to metabolize TGNPs by HeLa cells.

CONCLUSION

In summary, with DWVD, the tempo-spatially resolved cellular dynamics of drug delivery nanocargo, TGNPs, were explored in living HeLa cells. It was found that energy-dependent endocytosis (both clathrin and caveolae mediated processes were involved) was the dominant pathway for the HeLa cells' uptake of TGNPs. The single particle tracking experiments on living cell membrane revealed unusual hop diffusions, which is remarkably different from the dynamics in the control experiment (CTAB modified gold nanoparticle). Alternatively, this kind of movement is reminiscent of the behavior of ligand-modified nanocargo (such as transferrin) on living cell membrane. Based on the time-correlated dynamic spatial distribution information, it was found that TGNPs could not actively target cell nuclei, which is contrary to previously proposed conclusion based on fixed cell results. Motor proteins directed movement was the essential source to drive TGNPs transporting in HeLa cells. More importantly, propagation of TGNPs to the daughter cells through mitosis was found to be the sole pathway to dilute (or exclude) them in living cells.

Although above knowledge is elucidated from a model system (i.e. spherical gold nanoparticles and HeLa cells), this work can, in principle, provide several important insights for the rational design of high efficient drug carriers with CPPs. For example, to improve the drug action, additional stimuli mechanisms are suggested to adopt to trigger drug release from the endocytic vesicles such as pH change, light, and temperature changes. To achieve subcellular targeting capability, other signaling molecules are recommended to further attach on the nanocargo surface. The dosage of nanocargo applied in the treatment is also an important concern from the consideration of the metabolizing mechanism as noted above. Furthermore, because of the versatility of DWVD, this living cell imaging platform would display broad potentials in the exploration of dynamic nanoparticle-cell interaction mechanisms in living cells in the future.

ASSOCIATED CONTENT

Supporting Information. Experimental section and additional supporting results as noted in the text. This material is available free of charge via the Internet.

AUTHOR INFORMATION

Corresponding Author

E-mail: lehuixiao@gmail.com

Notes

The authors declare no competing financial interests.

ACKNOWLEDGMENT

This work was supported by NSFC (21205037, 20927005, 21275049), Program for New Century Excellent Talents in University (China, NCET-13-0789), Hunan Natural Science Funds for Distinguished Young Scholar (14JJ1017), and the aid program for science and technology innovation research team in higher education institutions of Hunan Province.

Figures and captions:

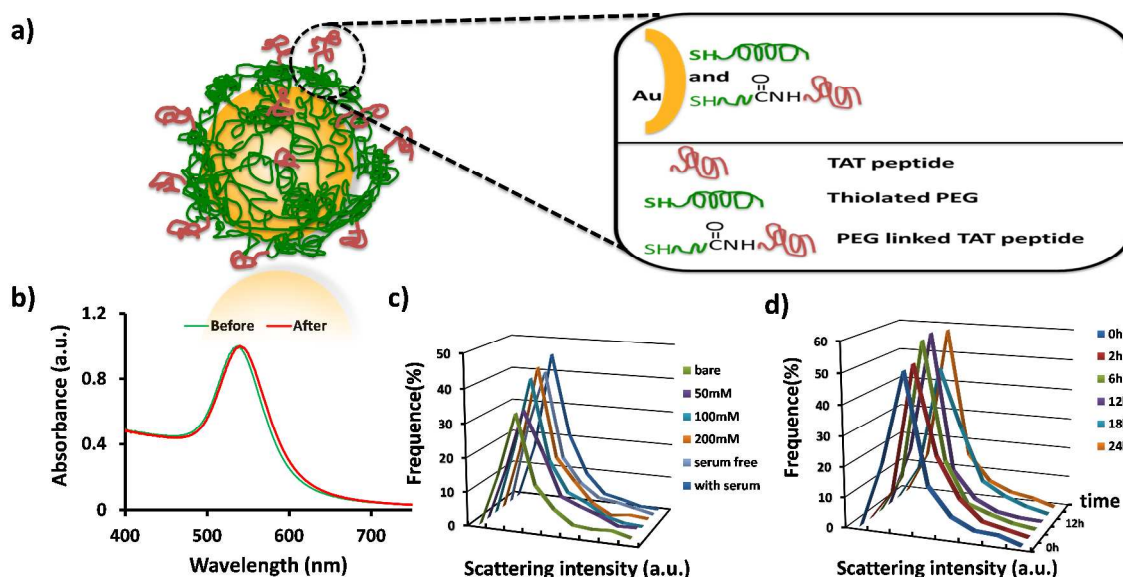


Figure 1. a) schematic diagram of TGNPs functionalization. b) UV-vis absorption spectra of 60 nm gold nanoparticles (green) and TGNPs (red). c) from front to back are the scattering intensity distributions of single gold nanoparticles in water, TGNPs in 50, 100, 200 mM sodium chloride solution and cell culture medium without and with serum respectively. d) from front to back are scattering intensity distributions of TGNPs in serum-free cell culture medium with incubation time of 0h, 2h, 6h, 12h, 18h and 24 h respectively.

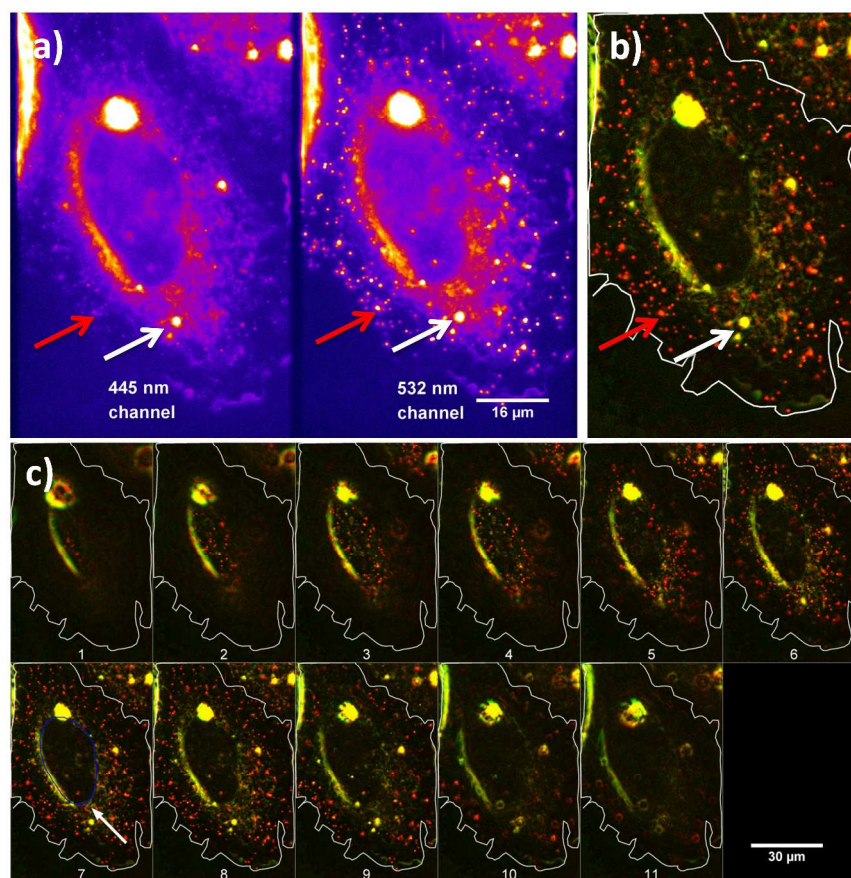


Figure 2. a) typical DWVD image of single HeLa cell co-incubated with TGNPs at 37 °C for 0.5 h. The scattering images from 445 nm and 532 nm channels are shown in the left and right sides, respectively. Due to the plasmon resonance effect, the scattering efficiency of TGNPs in 532 nm channel is notably higher than that in 445 nm channel. By merging the images from 445 nm (using green color) and 532 nm (using red color) channels into a single color-coded image, the noise from cellular organelles (white arrow, orange spot in the merged image) can therefore be effectively distinguished from TGNPs (red arrow, red spot in the merged image) as shown in b). c) the corresponding color-coded three dimensional section images of HeLa cell from top to down with stepping size around 300 nm.

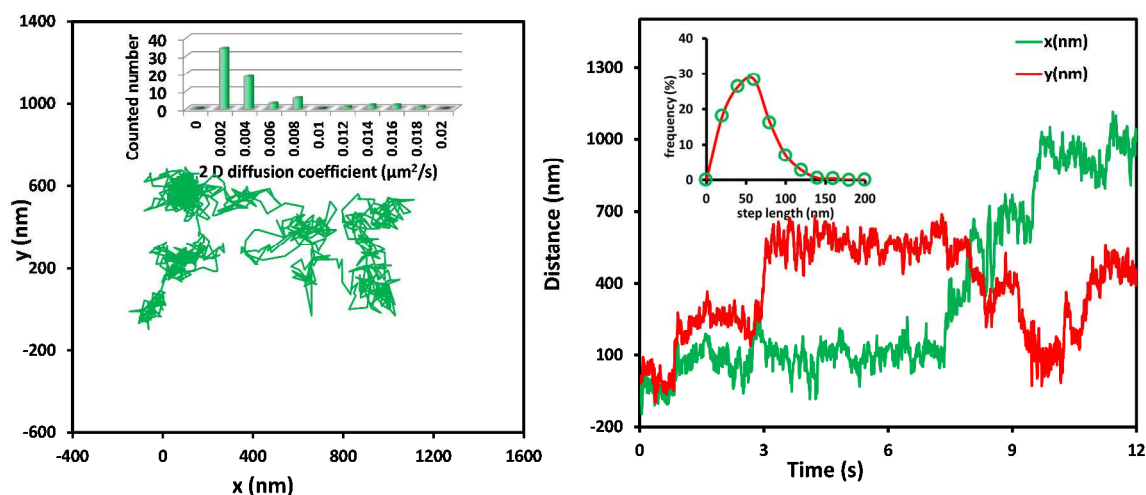


Figure 3. a) representative diffusion trajectory of single TGNP on HeLa cell membrane. Inserted is the distribution of two dimensional diffusion coefficients of TGNPs on HeLa cell membrane. b) the corresponding one dimensional trajectories in x (green) and y (red) directions respectively. Inserted plot is the statistical analysis of two-dimensional step size from 68 TGNPs.

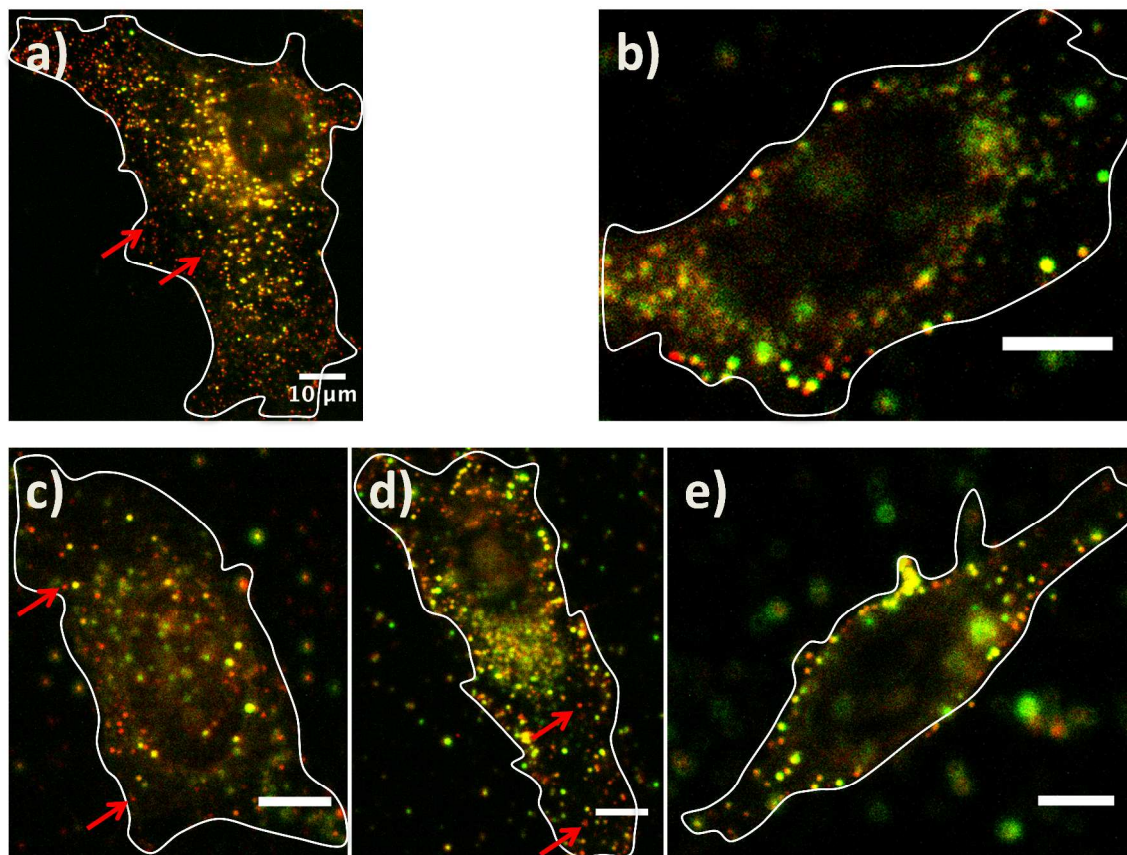


Figure 4. a) and b) are the color-coded two channel merged images of HeLa cells co-incubated with TGNPs at 37 °C and 4 °C respectively. Typical TGNPs are indicated with red arrows. From c) to e) are the biochemical inhibitor studies by treating HeLa cells with Dynasore, genistein, and both of them respectively. Scale bar 10 μm .

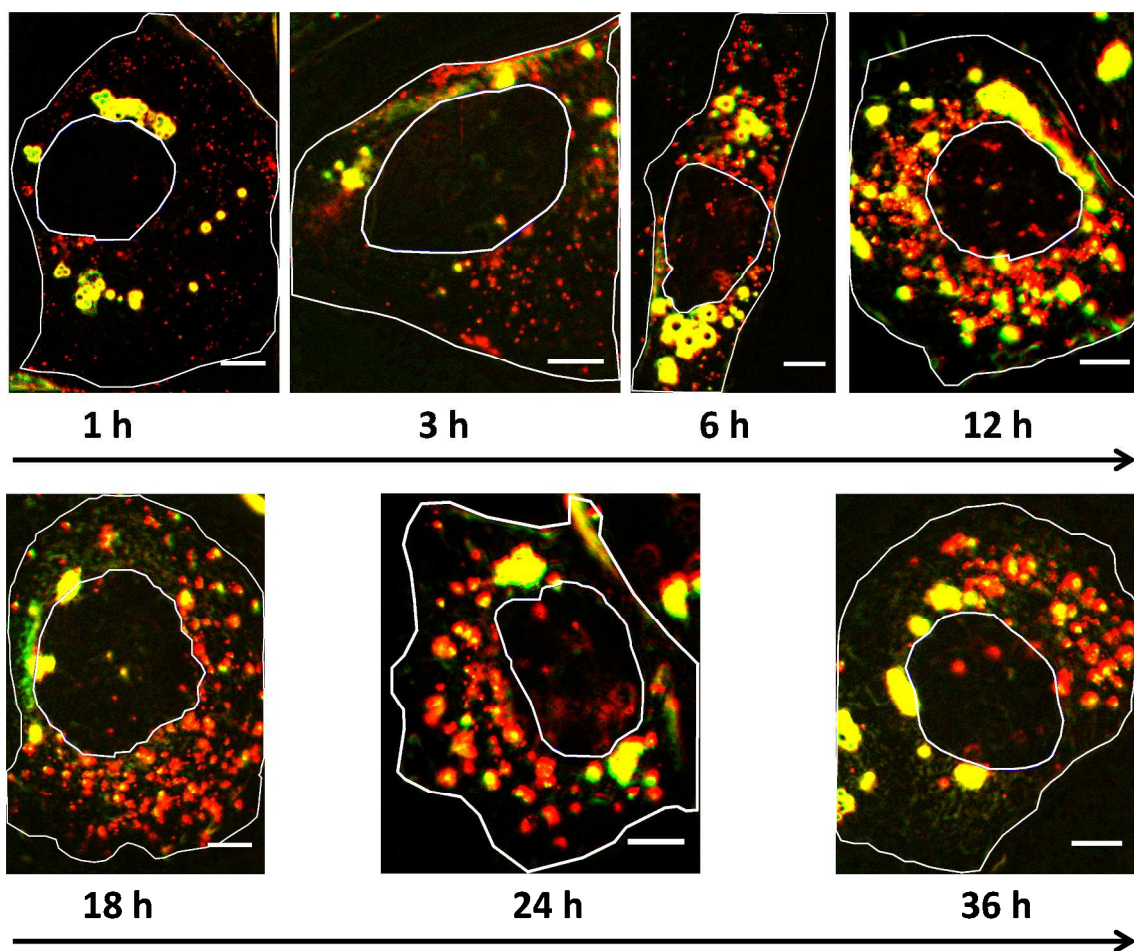


Figure 5. Intracellular distributions of TGNPs in HeLa cells as a function of time. The edges of cell membrane and nuclei are marked with white lines. Scale bar 10 μm .

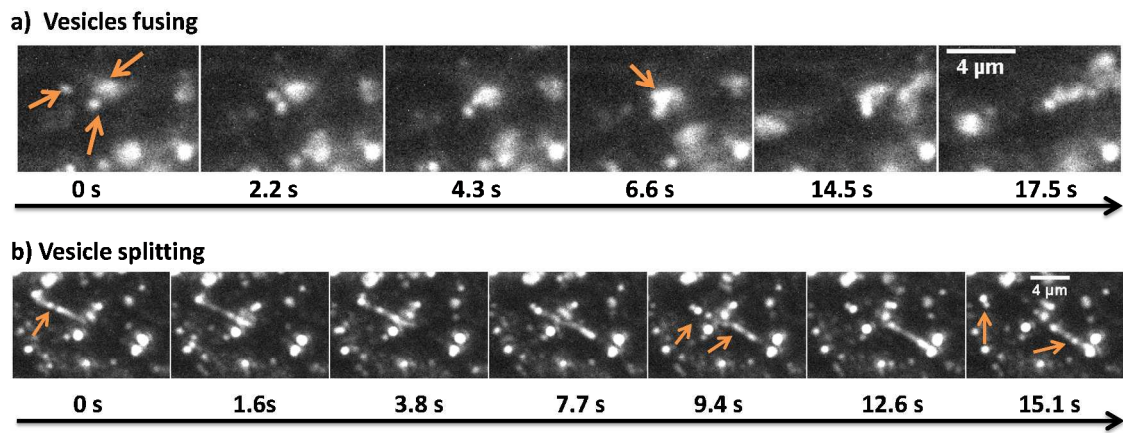


Figure 6. Motor proteins guided vesicles fusing (a) and splitting (b) on cell cytoskeletons.

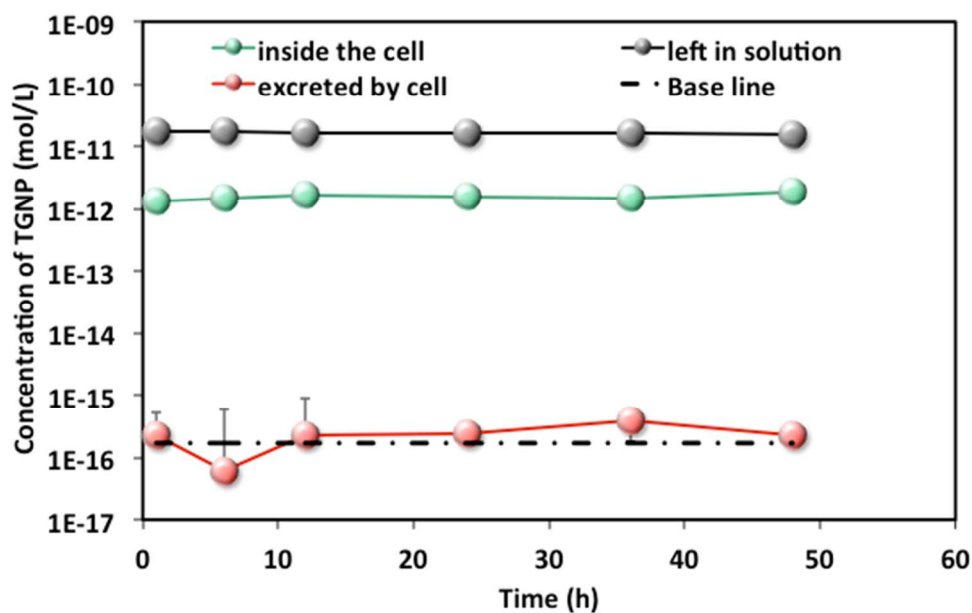


Figure 7. Atomic absorption spectrum measurements of TGNPs content within HeLa cells (green dots) as a function of time by co-incubating TGNPs with HeLa cells for 1 h and then washed out those left in cell culture medium (gray dots). Those TGNPs excreted by cells at different time points are shown with red dots.

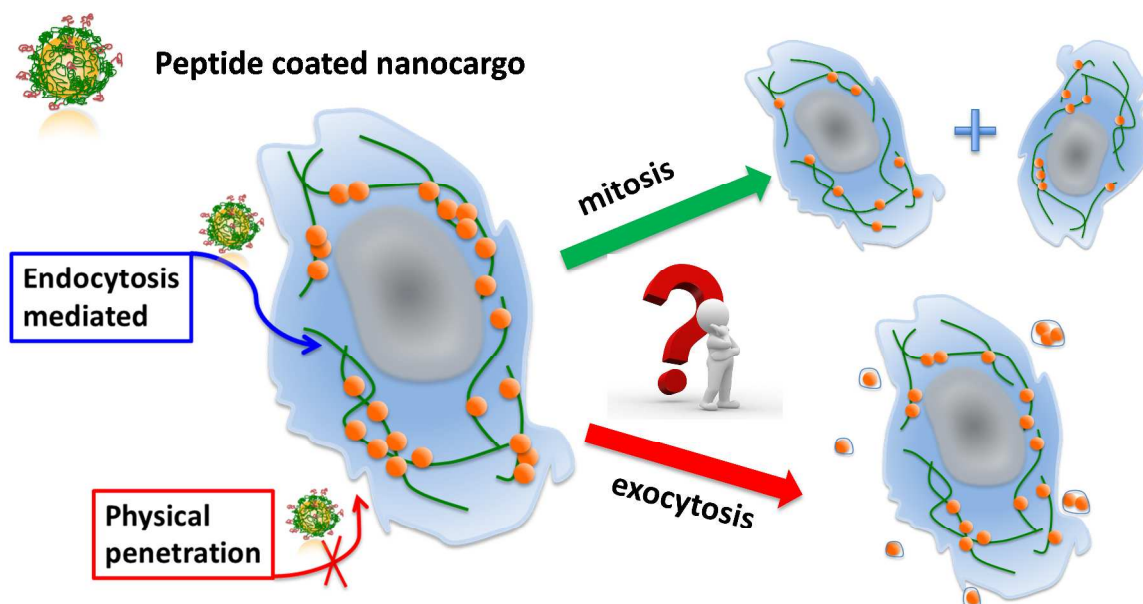
REFERENCES

1. B. S. Wong, S. L. Yoong, A. Jagusiak, T. Panczyk, H. K. Ho, W. H. Ang, and G. Pastorin, *Adv. Drug Deliv. Rev.*, 2013, **65**, 1964–2015.
2. Y. Malam, M. Loizidou, and A. M. Seifalian, *Trends Pharmacol. Sci.*, 2009, **30**, 592–599.
3. I. I. Slowing, B. G. Trewyn, S. Giri, and V. S.-Y. Lin, *Adv. Funct. Mater.*, 2007, **17**, 1225–1236.
4. P. Ghosh, G. Han, M. De, C. K. Kim, and V. M. Rotello, *Adv. Drug Deliv. Rev.*, 2008, **60**, 1307–1315.
5. E. C. Dreaden, A. M. Alkilany, X. Huang, C. J. Murphy, and M. A. El-Sayed, *Chem. Soc. Rev.*, 2012, **41**, 2740–2779.
6. S. Eustis and M. A. El-Sayed, *Chem. Soc. Rev.*, 2006, **35**, 209–217.
7. C. J. Murphy, A. M. Gole, J. W. Stone, P. N. Sisco, A. M. Alkilany, E. C. Goldsmith, and S. C. Baxter, *Acc. Chem. Res.*, 2008, **41**, 1721–1730.
8. N. L. Rosi, *Science*, 2006, **312**, 1027–1030.
9. G. Han, C.-C. You, B.-J. Kim, R. S. Turingan, N. S. Forbes, C. T. Martin, and V. M. Rotello, *Angew. Chem. Int. Ed.*, 2006, **45**, 3165–3169.
10. Y. D. Álvarez, J. A. Fauerbach, J. V. Pellegrotti, T. M. Jovin, E. A. Jares-Erijman, and F. D. Stefani, *Nano Lett.*, 2013, **13**, 6156–6163.
11. A. C. Bonoiu, S. D. Mahajan, H. Ding, I. Roy, K. T. Yong, R. Kumar, R. Hu, E. J. Bergey, S. A. Schwartz, and P. N. Prasad, *Proc. Natl. Acad. Sci. U.S.A.*, 2009, **106**, 5546–5550.
12. E. C. Cho, L. Au, Q. Zhang, and Y. Xia, *Small*, 2010, **6**, 517–522.
13. S. E. Gratton, P. A. Ropp, P. D. Pohlhaus, J. C. Luft, V. J. Madden, M. E. Napier, and J. M. DeSimone, *Proc. Natl. Acad. Sci. U.S.A.*, 2008, **105**, 11613–11618.
14. J. Rejman, V. Oberle, I. S. Zuhorn, and D. Hoekstra, *Biochem. J.*, 2004, **377**, 159–169.
15. W. Jiang, B. Y. S. Kim, J. T. Rutka, and W. C. W. Chan, *Nat. Nanotech.*, 2008, **3**, 145–150.
16. M. Zorko and U. Langel, *Adv. Drug Deliv. Rev.*, 2005, **57**, 529–545.
17. S. B. Fonseca, M. P. Pereira, and S. O. Kelley, *Adv. Drug Deliv. Rev.*, 2009, **61**, 953–964.
18. L. N. Patel, J. L. Zaro, and W.-C. Shen, *Pharm. Res.*, 2007, **24**, 1977–1992.
19. J. P. Richard, K. Melikov, E. Vivès, C. Ramos, B. Verbeure, M. J. Gait, L. V. Chernomordik, and B. Lebleu, *J. Biol. Chem.*, 2003, **278**, 585–590.
20. B. Gupta, T. S. Levchenko, and V. P. Torchilin, *Adv. Drug Deliv. Rev.*, 2005, **57**, 637–651.
21. M. C. Morris, J. Depollier, J. Mery, F. Heitz, and G. Divita, *Nat. Biotechnol.*, 2001, **19**, 1173–1176.
22. M. Mäe and U. Langel, *Curr. Opin. Pharmacol.*, 2006, **6**, 509–514.
23. S. Fawell, J. Seery, Y. Daikh, C. Moore, L. L. Chen, B. Pepinsky, and J. Barsoum, *Proc. Natl. Acad. Sci. U.S.A.*, 1994, **91**, 664–668.
24. H. Yuan, A. M. Fales, and T. Vo-Dinh, *J. Am. Chem. Soc.*, 2012, **134**, 11358–

- 11361.
25. J. M. de la Fuente and C. C. Berry, *Bioconjug. Chem.*, 2005, **16**, 1176–1180.
 26. Z. Krpetić, S. Saleemi, I. A. Prior, V. Sée, R. Qureshi, and M. Brust, *ACS Nano*, 2011, **5**, 5195–5201.
 27. I. M. Kaplan, J. S. Wadia, and S. F. Dowdy, *J. Control. Release*, 2005, **102**, 247–253.
 28. C. Ciobanasu, J. P. Siebrasse, and U. Kubitscheck, *Biophys. J.*, 2010, **99**, 153–162.
 29. F. Madani, S. Lindberg, U. Langel, S. Futaki, and A. Gräslund, *J Biophys*, 2011, **2011**, 414729.
 30. A. H. Faraji and P. Wipf, *Bioorg. Med. Chem.*, 2009, **17**, 2950–2962.
 31. H. Yuan, A. M. Fales, and T. Vo-Dinh, *J. Am. Chem. Soc.*, 2012, **134**, 11358–11361.
 32. E. Ruoslahti, S. N. Bhatia, and M. J. Sailor, *J. Cell Biol.*, 2010, **188**, 759–768.
 33. L. Rajendran, H.-J. Knölker, and K. Simons, *Nat. Rev. Drug Discov.*, 2010, **9**, 29–42.
 34. G. Ruan, A. Agrawal, A. I. Marcus, and S. Nie, *J. Am. Chem. Soc.*, 2007, **129**, 14759–14766.
 35. A. Mishra, G. H. Lai, N. W. Schmidt, V. Z. Sun, A. R. Rodriguez, R. Tong, L. Tang, J. Cheng, T. J. Deming, D. T. Kamei, and G. C. L. Wong, *Proc. Natl. Acad. Sci. U.S.A.*, 2011, **108**, 16883–16888.
 36. P. Nativo, I. A. Prior, and M. Brust, *ACS Nano*, 2008, **2**, 1639–1644.
 37. L. Wei, X. Zhao, B. Chen, H. Li, L. Xiao, and E. S. Yeung, *Anal. Chem.*, 2013, **85**, 5169–5175.
 38. A. G. Tkachenko, H. Xie, Y. Liu, D. Coleman, J. Ryan, W. R. Glomm, M. K. Shipton, S. Franzen, and D. L. Feldheim, *Bioconjug. Chem.*, 2004, **15**, 482–490.
 39. E. Oh, J. B. Delehanty, K. E. Sapsford, K. Susumu, R. Goswami, J. B. Blanco-Canosa, P. E. Dawson, J. Granek, M. Shoff, Q. Zhang, P. L. Goering, A. Huston, and I. L. Medintz, *ACS Nano*, 2011, **5**, 6434–6448.
 40. L. Xiao, L. Wei, X. Cheng, Y. He, and E. S. Yeung, *Anal. Chem.*, 2011, **83**, 7340–7347.
 41. B. D. Chithrani and W. C. W. Chan, *Nano Lett.*, 2007, **7**, 1542–1550.
 42. B. D. Chithrani, A. A. Ghazani, and W. C. W. Chan, *Nano Lett.*, 2006, **6**, 662–668.
 43. M. A. van Dijk, A. L. Tchegotareva, M. Orrit, M. Lippitz, S. Berciaud, D. Lasne, L. Cognet, and B. Lounis, *Phys. Chem. Chem. Phys.*, 2006, **8**, 3486–3495.
 44. L. Xiao, L. Wei, Y. He, and E. S. Yeung, *Anal. Chem.*, 2010, **82**, 6308–6314.
 45. X. Nan, P. A. Sims, and X. S. Xie, *ChemPhysChem*, 2008, **9**, 707–712.
 46. C. Ciobanasu, E. Harms, G. Tünnemann, M. C. Cardoso, and U. Kubitscheck, *Biochemistry*, 2009, **48**, 4728–4737.
 47. L. Xiao, L. Wei, C. Liu, Y. He, and E. S. Yeung, *Angew. Chem. Int. Ed.*, 2012, **51**, 4181–4184.
 48. G. J. Doherty and H. T. McMahon, *Annu. Rev. Biochem.*, 2009, **78**, 857–902.
 49. E. Macia, M. Ehrlich, R. Massol, E. Boucrot, C. Brunner, and T. Kirchhausen, *Dev. Cell.*, 2006, **10**, 839–850.
 50. L. Xiao, R. Zhou, Y. He, Y. Li, and E. S. Yeung, *J. Phys. Chem. C*, 2009, **113**, 1209–1216.
 51. R. Matteoni and T. E. Kreis, *J. Cell Biol.*, 1987, **105**, 1253–1265.

52. C. Brandenberger, C. Mühlfeld, Z. Ali, A.-G. Lenz, O. Schmid, W. J. Parak, P. Gehr, and B. Rothen-Rutishauser, *Small*, 2010, **6**, 1669–1678.

TOC



With a dual wavelength view darkfield (DWVD) microscope, the tempo-spatially resolved dynamics of Tat peptide-functionalized gold nanoparticles (TGNPs) in living HeLa cells were studied. Energy-dependent endocytosis (both clathrin and caveolae mediated processes were involved) was found to be the prevailing pathway for the cellular uptake of TGNPs. The time-correlated dynamic spatial distribution information revealed that TGNPs could not actively target the cell nuclei and inheritance of TGNPs to the daughter cells through mitosis was the major route to metabolize TGNPs by HeLa cells.